Computer Simulation of Static and Dynamic Behavior of Diblock Copolymer Melts

T. Pakula*

Max-Planck-Institut für Polymerforschung, P.O. Box 3148, D-55021 Mainz, Germany

K. Karatasos, S. H. Anastasiadis,† and G. Fytas

Foundation for Research and Technology−Hellas, Institute of Electronic Structure and Laser, P.O. Box 1527, 711 10 Heraklion Crete, Greece

Received April 3, 1996; Revised Manuscript Received September 11, 1997[⊗]

ABSTRACT: Monte Carlo simulations, using the cooperative motion algorithm (CMA), have been employed to investigate the statics and dynamics of both symmetric and asymmetric diblock copolymer melts near the order−disorder transition. Investigation of the static properties has revealed the existence of two characteristic temperatures in the system: the ODT expressed as a peak in the heat capacity and a higher temperature T_1 at the crossover between the homogeneous state and the state with considerably increased concentration fluctuations. As T_1 is crossed, the increased amplitude of concentration fluctuations is accompanied by a significant increase of the average end-to-end distance of chains and the local chain orientation correlation. The dynamic properties of these systems have been observed by means of the relaxation of the single-bond, the chain end-to-end vector, and the block end-to-end vector, as well as by the single point concentration autocorrelation function. Corresponding relaxation times have been determined as a function of temperature. Below the ODT, a splitting of both the chain and the block end-to-end vector orientation correlation function is observed, while the relaxation of composition fluctuations becomes slower than that of the block orientation. The slow process is attributed to the conformal relaxation of the coherent interfaces formed in the ordered state.

I. Introduction

Diblock copolymers, consisting of two linear sequences of chemically different species A and B, represent an interesting class of polymeric materials with a rich variety of phase behavior.[1] This makes them a subject of interest in experiments,[1−6] theory,[7−12] and computer simulations.[13−16] Relevant parameters controlling the phase behavior of such systems are the overall degree of polymerization, N, the volume fraction of the A block, f, and the interaction parameter, χ, related to direct interaction between species A and B. Depending on the product χN, various states are distinguished in such systems ranging between homogeneous or disordered states at low values of χN and a microphase-separated state at high χN, with an order−disorder transition separating these regimes at $\chi N \approx 10$. The ordered states are characterized by a long range order exceeding the molecular sizes and various morphologies depending on f. Up to now, most of the scientific interest has been devoted to static properties of such systems. Only recently, the dynamics of diblock copolymers, and the influence of the order−disorder transition on the dynamics have attracted the increased interest of polymer scientists, both experimentally[17−26] and theoretically.[26−32]

Computer simulations have also provided results[13−16] concerning mainly static properties of block copolymers. Binder and Fried performed Monte Carlo lattice simulations in three dimensions for both symmetric[13] and asymmetric[14] diblocks using a slithering snake algorithm. This was accomplished by introducing vacancies occupying a volume fraction of $f_v = 0.2$ in the lattice. The ODT was located in the temperature range where the correlation time of the structure factor $S(\mathbf{q})$ in the disordered state ($\mathbf{q}$ is the wave vector) shows a significant slowing down. The ODT was found to lie between the Leibler[7] and Fredrickson−Helfand[8] predictions. Furthermore, the average conformational state of the individual copolymer chains revealed significant deviation from the Gaussian behavior exemplified by an increase of the radius of gyration by 10−15%, as the ODT was approached from the disordered state. Pakula and co-workers[15] utilized the cooperative motion algorithm (CMA) to investigate the ordering phenomena for symmetric diblocks in dense polymer systems, i.e., $f_v = 0$. Using a much faster simulation method, they were able to observe the systems in both the disordered and ordered states. The ODT was identified from an analysis of the specific heat of the copolymer melt and was nearly in agreement with the predictions of the fluctuation theory.[8] The copolymer chains displayed conformational behavior similar to that seen in the simulations of Binder[13,14] and an orientation correlation occurring at temperatures near the ODT. Larson[16] performed Monte Carlo simulations for symmetric diblocks on a cubic lattice where a qualitative change in the order−disorder transition behavior was observed when the number of segments in the molecule exceeds 50. For shorter chains the fluctuations near the transition are short-ranged and the order parameter in the ordered state at the transition is high, whereas for longer chains fluctuations that are correlated over multiple lamellae become important and the order parameter on the ordered side of the transition is small, in agreement with the weak segregation theories.

In this work, we attempt an investigation of the molecular dynamics in diblock copolymer melts in a broad temperature range including both the disordered and the ordered state. Dynamic Monte Carlo simulations using the cooperative motion algorithm (CMA) are employed to investigate the statics and dynamics in melts of both symmetric and asymmetric diblock copolymers. It has already been demonstrated that the

* To whom correspondence should be addressed.
† Also at Physics Department, University of Crete, 711 10 Heraklion Crete, Greece.
⊗ Abstract published in *Advance ACS Abstracts,* December 1, 1997.

S0024-9297(96)00510-4 CCC: $14.00

CMA, which is the only algorithm that can operate in really dense lattice melts of polymers, is very effective for the simulation of block copolymers.[15] It allows us to study such systems over a broad temperature range including the regions on both sides of microphase separation. In this paper, we examine again systems representing diblock copolymer melts, as described before[15] but paying particular attention now to their dynamic behavior. The CMA has been used earlier to study dynamic problems in homopolymer melts.[33−36] Results obtained have indicated that this simulation method reflects a behavior of linear polymer chains that is in good agreement with experimental observations.[35,36]

This article is arranged as follows: The methodology of the Monte Carlo simulations is presented in the next section (II). In section III static and dynamic properties of the simulated systems are shown. Predictions of the simulation are discussed in relation to experimental data and theoretical calculations in section IV. Finally, concluding remarks constitute section V.

II. Computer Simulations

Simulation Method. The cooperative motion algorithm (CMA) permits one to simulate dense polymer melts on a lattice.[33−36] The lattice is completely occupied by monomers, and the monomers of each chain are connected by $(N - 1)$ bonds of constant length a. The chains satisfy the excluded volume condition. In the case of copolymers two types of monomers A and B are considered. The two types of monomers are partially compatible, which is characterized by direct interaction parameters ϵ_{ij}. The energy of mixing is determined only by the interactions of monomers of different types; therefore, we assume here that $\epsilon_{AA} = \epsilon_{BB} = 0$ and $\epsilon_{AB} = 1$. The effective energy of one monomer E_n, given by the sum of ϵ_{AB} over z nearest neighbors, will depend on the local structure.

In order to generate equilibrium states, a dense system of chains is subjected to motion at a given temperature. The moves are strictly cooperative, as in a dense system ($\rho = 1$), so that a segment of one chain can only move if other segments of different chains move simultaneously. Moving a chain element alters the local energy because the monomers contact new neighbors. An attempt to move a single monomer is assumed to define one Monte Carlo step and the probability of motion is related to the interaction energy of the monomer in the attempted position, which means that the repulsive interaction energy ϵ_{AB} is considered as a barier to form A−B contacts. The Metropolis method is not used because the dynamics of systems is of interest. At a given temperature, T, the Boltzmann factor $p = \exp(-E_{n,final}/k_BT)$ is compared with a random number r, $0 < r < 1$. If $p > r$, the move is performed and the motion of a new monomer is attempted. Since $\epsilon_{AB} > 0$, at low temperatures, the different types of monomeric units tend to separate from each other in order to reduce the number of A−B contacts and, consequently, to reduce the energy.

The simulations are performed on a face-centered cubic (fcc) lattice with bond length $a = \sqrt{2}$. The possible bond angles are $\alpha = 60$, 90, 120, and 180° with degeneracy $d_\alpha = 4$, 2, 4, and 1, respectively. The coordination number of the lattice is $z = 12$; i.e., every monomer has 12 nearest neighbors. The lattice dimensions are $30 \times 30 \times 40$ lattice sites. Periodic boundary conditions have been employed in order to reduce boundary effects.

Three different diblock copolymer systems have been considered: two symmetric diblocks with chain lengths $N = 20$ and $N = 40$ and $f = 0.5$ and an asymmetric diblock with $N = 40$ and $f = 0.25$. The system is initially equilibrated in the athermal limit, i.e., at $\epsilon_{ij}/(k_BT) = 0$ (k_B is the Boltzmann constant), where there are no interactions between monomers, except the excluded volume constraints. The systems are subsequently cooled to a temperature $T/N = 1.0$, by a temperature jump, and equilibrated again. Starting from such a configuration, the system is cooled slowly by small temperature steps. At each temperature the system is equilibrated and characterized by its energy and a number of quantities describing its static properties. The system cooled to a low temperature can be observed during heating in the same way. Quantities characterizing the system are calculated only between cooperative rearrangement steps.

Application of the CMA to study dynamics in copolymer systems is justified mainly by the success of this method in description of dynamic properties of homopolymer melts.[35,36] In this method only cooperative local rearrangements are considered as a result of dense packing and a necessity of preservation of the continuity of systems. The rearrangements involve local conformational changes within one polymer chain or in several neighboring chains, in all cases preserving the identity of chains given by chain lengths, sequences of monomers along the chains, and nonbreakability of bonds. There is a distribution of rearrangement sizes within this method that is a fast decreasing function with increasing rearrangement size (size distribution of random self-avoiding circuits on the lattice). In spite of the distribution of sizes, the rearrangements remain local and randomly distributed in space. This makes the algorithm suitable for studies of dynamic problems.

Calculated Quantities. The energy of interaction per monomer is calculated as a sum of direct interactions between a given monomer and its z nearest neighbors

$$E_n(T) = \sum_{i=1}^{z} \epsilon_{jk}(i) \tag{1}$$

where indices j and k can both be A or B, depending on the local configuration. The specific heat in the simulation has been obtained via the fluctuation dissipation theorem

$$c_v = \frac{1}{k_B T^2}(\langle E^2 \rangle - \langle E \rangle^2) \tag{2}$$

where the brackets denote averages computed during the simulation over the total energy of the system. The thermodynamic state of the system can also be characterized by the effective interaction parameter

$$\chi_{eff} = \frac{\frac{1}{2}\langle E_n \rangle}{k_B T \phi_A \phi_B} \tag{3a}$$

where T is temperature and ϕ_A and ϕ_B are the volume fractions of monomers of type A and B in the system, respectively. In the following, k_B is assumed to equal 1. This description of the interactions is introduced in order to be able to compare the actual state of interaction in the system, given by the number of contacts between A and B elements, with the Flory interaction

parameter[37] defined as

$$\chi_F = \frac{(z-2)\epsilon_{AB}}{k_B T} \tag{3b}$$

where z is the coordination number of the lattice (for the fcc lattice $z = 12$). The χ_F interaction parameter is considered as describing interactions in a homogeneously mixed state of the system.

In order to characterize the chain conformation, the end-to-end distance has been calculated

$$\langle R^2 \rangle = \frac{1}{n_s n_p} \sum_{n_s} \sum_{n_p} (r_N - r_1)^2 \tag{4}$$

where r_N and r_1 are space coordinates of monomers at chain ends. The averaging is performed over the ensemble of n_p chains and over n_s states of the system at equilibrium, sampled at constant time intervals. Typically $n_p > 300$ and $n_s > 1000$.

It has been observed in the former simulations of block copolymers,[15] in agreement with recent theroretical work,[31,32] that at the microphase separation transition the chains become orientationally correlated. Two orientation correlation functions of the end-to-end vectors are here determined in order to describe this effect: (1) the local orientation correlation given by the orientation factor

$$f_1 = \langle \cos[\theta_{RR}(r_{ij})] \rangle \quad \text{for} \quad r_{ij} \le \sqrt{\langle s^2 \rangle}; \quad i \neq j \tag{5}$$

where $\theta_{RR}(r_{ij})$ is the angle between the end-to-end vectors (oriented from the end of block A to the end of block B) of two chains whose centers of mass are separated by a distance r_{ij}, smaller than the root mean square radius of gyration of the corresponding unperturbed linear chains, $\langle s^2 \rangle$; and (2) the global orientation correlation of the system characterized by the orientation factor

$$f_{RR} = \frac{1}{2}(3\langle \cos^2(\theta_{ij}) \rangle - 1) \tag{6}$$

where the averaging is performed over all end-to-end vector pairs belonging to many states of the system in equilibrium.

Local concentration fluctuations are characterized by

$$\eta^2 = \langle (\phi_i - f)^2 \rangle \tag{7}$$

where f is the nominal composition of the system (for a symmetric system, $f = 0.5$), and ϕ_i is the local concentration determined for the nearest neighbor shell of each monomer.

In order to get information about the dynamic properties of systems, the following quantities have been monitored with time at equilibrium states corresponding to various temperatures: (i) the single bond autocorrelation function

$$\rho_b(t) = \frac{1}{N} \frac{1}{n_p} \sum_{n_p} \sum_{i=1}^{N} \mathbf{b}_i(t)\, \mathbf{b}_i(0) \tag{8}$$

where $\mathbf{b}_i$ are unit vectors representing bond orientation; (ii) the end-to-end vector autocorrelation function

$$\rho_R(t) = \frac{1}{n_p} \sum_{n_p} \mathbf{R}(t)\, \mathbf{R}(0) \tag{9}$$

with end-to-end vectors $\mathbf{R}(0)$ and $\mathbf{R}(t)$ at times $t = 0$ and t, respectively; (iii) the autocorrelation function of the end-to-end vector of the block

$$\rho_{bl}(t) = \frac{1}{n_p} \sum_{n_p} \mathbf{R}_{bl}(t)\, \mathbf{R}_{bl}(0) \tag{10}$$

with $\mathbf{R}_{bl}$ the end-to-end vector of one block; and (iv) the single point concentration correlation

$$\rho_c(t) = \frac{1}{n} \sum_{n} c(t)\, c(0) \tag{11}$$

with c assuming values $+1$ or -1 when the lattice site is occupied by monomer A or B, respectively.

The above correlation functions were analyzed in two ways: (1) by carrying out the inverse Laplace transformation (ILT) of the calculated $\rho(t)$ assuming a superposition of exponential functions and utilizing the CONTIN routine[38] as used often in analysis of photon correlation spectroscopy results[39]

$$\rho(t) = \int_{-\infty}^{\infty} L(\ln \tau) \exp(-t/\tau)\, d(\ln \tau) \tag{12}$$

and (2) by determination of the characteristic relaxation times by fitting a sum or stretched exponential functions

$$\rho(t) = \sum_i A_i \exp\left[-\left(\frac{t}{\tau_i}\right)^{\beta_i}\right] \tag{13}$$

where the number of components $i = 1$ or 2.

III. Simulation Results

Static Properties. Static and thermodynamic properties of simulated systems are analyzed here briefly in order to determine temperatures of phase transitions and characterize the related structural changes.

Former simulations of diblock copolymer systems have shown[15] that the microphase separation temperature can be determined from the temperature dependence of the energy of the system or the energy fluctuations, which allow one to determine the specific heat. In Figure 1, various thermodynamic quantities characterizing the system over a broad temperature range are shown. The interaction energy determined for the symmetric system with chain length $N = 40$ under heating is presented in Figure 1a. It was proven that the heating rate was slow enough to give a rate-independent shape of the energy curve. The specific heat (Figure 1b) has been determined according to eq 2, whereas the effective interaction parameter (Figure 1c) has been calculated from the energy values by means of eq 3a. All the temperature dependencies shown in Figure 1 suggest that two characteristic temperatures exist at which the thermodynamic quantities change in a specific way. The first characteristic point on the temperature scale, T_1, is assigned to the position of a broad step in the specific heat. When the system is cooled, the specific heat changes at T_1 from very small values above T_1 to some remarkably higher values below this temperature. At the same temperature, the interaction parameter χ_{eff} starts to deviate considerably from the dependence, which it obeys at high temperatures

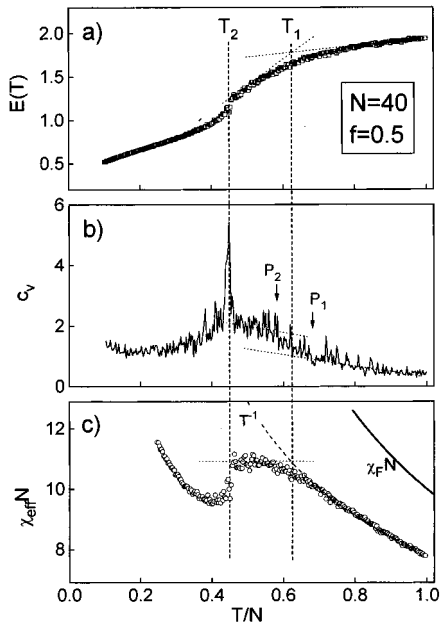

Figure 1. Temperature dependencies of various thermodynamic quantities determined for the simulated system of a symmetric diblock copolymer melt with chain length $N = 40$ and composition $f = 0.5$: (a) effective interaction energy per monomer $E(T)$; (b) specific heat at constant volume $C_v(T)$; (c) $\chi_{eff}N$ values, where χ_{eff} is the effective interaction parameter (see eq 3). The characteristic temperatures T_1 and T_2 are shown by vertical dashed lines. T_1 is located at the point where the extrapolated dependencies $\chi_{eff}N \propto T^{-1}$ and $\chi_{eff}N \cong$ const cross each other, corresponding also to the middle of the temperature interval between points P1 and P2 where the specific heat changes betweeen two different levels. T_2(ODT) is given by the jump in $E(T)$ and by the peak position of $C_v(T)$. The solid line in (c) shows the temperature dependence of $\chi_F N$, where χ_F is the Flory interaction parameter.

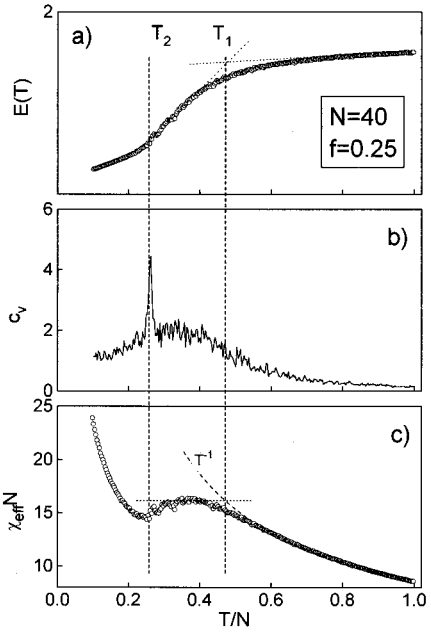

Figure 2. Temperature dependencies of various thermodynamic quantities determined for the simulated system of an asymmetric diblock copolymer melt with chain length $N = 40$ and composition $f = 0.25$: (a) effective interaction energy per monomer $E(T)$; (b) specific heat at constant volume $C_v(T)$; (c) $\chi_{eff}N$ values, where χ_{eff} is the effective interaction parameter. The characteristic temperatures T_1 and T_2, shown by vertical dashed lines, were estimated in the same way as in Figure 1.

Table 1. Characteristics of the Simulated Diblocks

N	N_A	N_B	f	T_1	T_2	$(\chi_{eff}N)_{ODT}$
40	20	20	0.50	0.62	0.45	10.9
20	10	10	0.50	0.65	0.46	11.1
40	10	30	0.25	0.47	0.26	16.1

($\chi_{eff} \propto T^{-1}$), toward a plateau at lower temperatures. The point, where the high temperature dependence ($\chi_{eff} \propto T^{-1}$) crosses the plateau level of $\chi_{eff}N$ at lower temperatures (Figure 1c), is taken as T_1, in order to mark approximately a broad region of a crossover between two different types of behavior. The second characteristic temperature T_2 is assigned to the stepwise change in the energy and corresponding peak in the specific heat. This temperature is further regarded as the temperature of the order−disorder transition, T_{ODT}. The change in the behavior at T_1 will be regarded as a crossover between the homogeneous state and the state with considerably increased concentration fluctuations. Exactly the same behavior has been observed for the lower molecular weight symmetric diblock ($N = 20$, $f = 0.5$). Similar behavior is also shown in Figure 2 for the asymmetric system ($N = 40$, $f = 0.25$). As expected,[7,8] T_2 is observed at temperatures lower than for the symmetric system. The same also holds for the temperature T_1. The thermodynamic parameters at both temperatures are summarized in Table 1 for the two symmetric and the asymmetric diblock. A weak chain length dependence of T/N and χN values is evident for the two symmetric diblocks, which is probably due to the change in the importance of fluctuation effects with a change in the molecular weight.[8]

Figure 3 shows the temperature dependencies of various parameters characterizing the structure of the symmetric system. It is seen that all these quantities change in a characteristic way at temperatures T_1 and T_2. Above the temperature T_1, the system can be regarded as a homogeneous single phase because the structure characteristic for athermal conditions is almost preserved. This situation changes at T_1 where the local concentration fluctuations start to increase with decreasing temperature (Figure 3a). At the same time the chains start to extend (Figure 3b) and become locally orientationally correlated, as revealed by f_1 (eq 5) determined for chains separated by distances smaller than the radius of gyration (Figure 3c). Within the temperature range between T_1 and T_2 a continuous increase of the amplitude of concentration fluctuations, of the extension of chains, and of the local chain−chain orientation correlation is observed. At T_2 a drastic change in all these quantities is indicated by a sudden jump corresponding to the jump observed in the temperature dependence of energy (Figure 1a). Below T_2 all quantities determined change only slowly and indicate a tendency to assume plateau values extending to low temperatures. It is interesting to notice the difference in behavior of the local and global orientation correlation factors (Figure 3c). Locally, the chains become orientationally correlated at T_1, whereas the global orientation correlation factor remains 0 down to T_2, where it jumps suddenly to almost finite values. It indicates that the transition at T_2 is indeed related to the jump in the range of orientational order by the formation of coherent microdomains.

Figure 4 shows temperature dependencies of the same structural parameters determined for the asymmetric diblock copolymer. Except for a considerable shift of temperatures T_1 and T_2, the asymmetric diblock system shows a behavior similar to that of the symmetric one. The difference between the two systems is observed,

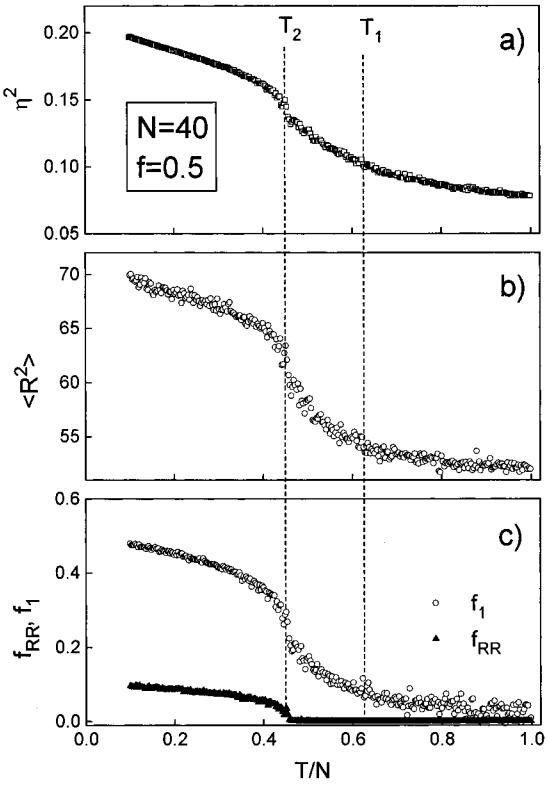

Figure 3. Temperature dependencies of various structural parameters characterizing the simulated system of a symmetric diblock copolymer melt with chain length $N = 40$ and composition $f = 0.5$: (a) mean-squared concentration fluctuation within the small volume element that includes nearest neighbors of a monomer; (b) mean-squared end-to-end distance of chains; (c) parameters f_1 and f_{RR} characterizing orientation correlations between end-to-end vectors of chains on local and long range scales, respectively.

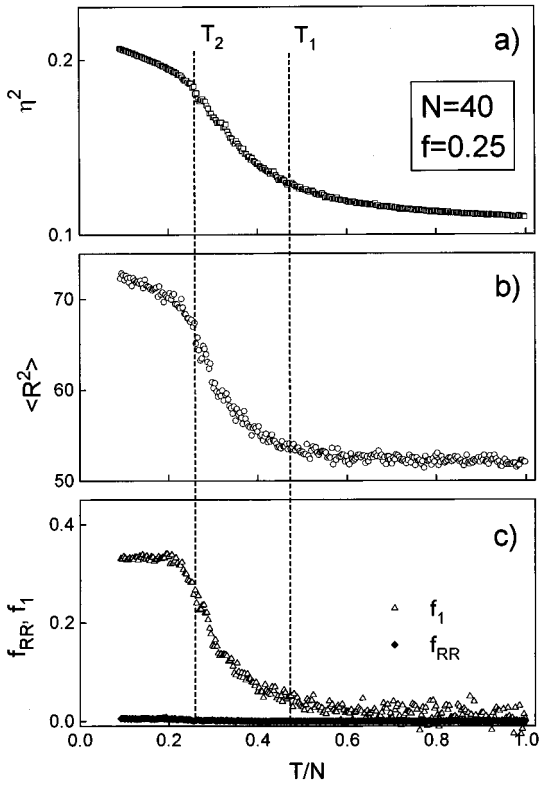

Figure 4. Temperature dependencies of various structural parameters characterizing the simulated system of the asymmetric diblock copolymer melt with chain length $N = 40$ and composition $f = 0.25$: (a) mean-squared concentration fluctuation within the small volume element that includes nearest neighbors of a monomer; (b) mean-squared end-to-end distance of chains; (c) parameters f_1 and f_{RR} characterizing orientation correlations between end-to-end vectors of chains on local and long range scales, respectively.

however, in the morphology formed below T_2. In the asymmetric diblock system ($f = 0.25$) a cylindrical morphology is formed, as can be observed in Figure 5b, in contrast to the lamellar morphology of the symmetric diblock (Figure 5a). The cylindrical microdomains in the case of the asymmetric diblock do not lead to macroscopic orientation correlation of chains in spite of the strong local correlation of chain orientations. This effect, well seen in the behavior of f_{RR} below T_2, is certainly related to differences in the microstructure formed in symmetric and asymmetric copolymer systems. In the case of lamellar microstructure, f_{RR} reflects orientation correlation of interface normals within a lamellar stack. In the case of cylindrical microdomains such correlation cannot be observed because of curved interfaces and corresponding axial symmetry of chain orientations within single cylinders.

A qualitative impression about the changes in the structure can be obtained from projections of the simulated systems, as shown in Figure 5, for various temperatures (a color contrast between monomers of types A and B is introduced). The increasing concentration fluctuations below T_1 upon cooling and the transition to the lamellar structure for the symmetric copolymer and the cylindrical structure for the asymmetric one at T_2 is well illustrated.

Taking the above information into account, we can conclude that at T_1 a crossover from the disordered phase characteristic for high temperatures to the weekly segregated states with increasing local order and increasing concentration fluctuations takes place. At T_2, the first-order transition transforms the system from a weekly segregated state to the ordered lamellar or cylindrical morphology extending over long distances.

Dynamic Properties. In Figure 6 examples of various correlation functions determined at temperatures corresponding to various structural states of the symmetric ($N = 40$) system both above and below the ODT are illustrated. Correlation functions characterizing relaxation of monomers (ρ_b), whole chains (ρ_R), and blocks (ρ_{bl}) as well as the relaxation of concentration (ρ_c) at various temperatures are shown.

At high temperatures, far above T_1, the system behaves like a homogeneous melt. All correlation functions, except for the point concentration correlation show a single step relaxation. The fastest is naturally the bond relaxation. Two modes of relaxation can be distinguished in the point concentration correlation (see also the relaxation time spectra in Figure 7d). The fast one should be attributed to the self-diffusion of the copolymer chains, as will become evident by its temperature dependence, as well. The slower mode of relaxation of point concentration fluctuations should be attributed to the relative motion of one block with respect to the other, the so-called internal mode.[24,25,27] The longest relaxation time is related to the end-to-end vector relaxation, whereas the block relaxation remains faster than the chain relaxation by about a factor of 2.

This dynamic picture changes when the system moves to temperatures below T_1. The bond and chain relaxations remain almost unaltered, but the block relaxation remarkably broadens or becomes a two-step function at

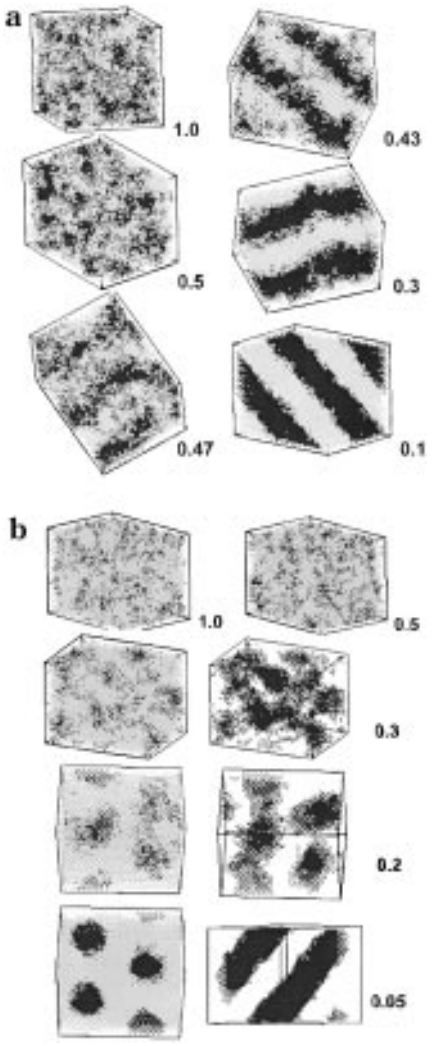

Figure 5. Snapshots of the real space morphology of the simulated (a) symmetric and (b) asymmetric diblock copolymer melts for temperatures above and below the ODT. A color contrast between monomers of type A and B has been introduced, whereas the bonds have been omitted for a better overview. At high temperatures, the melt is homogeneously mixed, as the temperature decreases, composition fluctuations are clearly seen, at the ODT, a lamellar (a) or cylindrical (b) structure is formed, and at even lower temperatures, a long range periodic morphology is observed. In (b) two representations of models with both components and with the minor component only are shown on the left and right hand side of the figure, respectively. At the two lowest temperatures the two cases correspond to two different projections of the system.

temperatures close to T_2 (compare also the relaxation time spectra in Figure 7c), The slow mode of the concentration relaxation becomes the slowest in the system. The broadening and the bifurcation of the block relaxation can be related to correlation of chain positions to quasi-interfaces that start to form between the regions of increasing concentration correlation of different compositions. The block-orientation relaxation has two components. The faster component is mainly related to the longitudinal and faster but limited orientational relaxation of the block within the microenvironment it prefers. The slower component of the relaxation is related to the relaxation of the quasi-interface to which the block feels anchored. The fast relaxation process of concentration fluctuations is not significantly altered by the decrease of temperature, whereas the slow mode shows a significant slowing down as the ODT (temperature T_2) is approached. The slowed down relaxation of the concentration is related to the increase of concentration correlation length and consequently higher stability of these correlations.

There is a further dynamic change in the dynamics at T_2. At this temperature the chain relaxation becomes also a two-step function where the fast component shows the part of chain relaxation that is given by the limited freedom of chains when fixed at the A−B interface and the slow component indicates the part of orientational chain relaxation that is coupled to the rate of relaxation of the interface and should depend on the sizes of ordered microphase-separated grains. The slower component can depend in this way on the kinetics of the phase separation and can become so slow that the relaxation time shifts away from the calculation time window. At these temperatures the block relaxation behaves in a way similar to that of the whole chain. The amplitude of the fast component of the concentration relaxation decreases, and the long time relaxation is also related to grains of coherently ordered microdomains. The slow component of chain and consequently block relaxations can be faster than the concentration relaxation because even passing through T_2 the chains preserve high mobility, however, trapped at the interfaces. They can move freely laterally within the interfaces (this effect will be described in detail elsewhere).

The effects described above can also be represented by changes of distributions of relaxation times with temperature. The distributions can be given by the inverse laplace transformation (ILT) of corresponding correlation functions. Some characteristic examples of the distributions are shown in Figure 7 for the symmetric and in Figure 8 for the asymmetric copolymer, respectively. In both figures the relaxation time distributions describing the behavior of systems at temperatures close to the ODT are plotted by thick solid lines. Generally, these dependencies separate the two different types of dynamic behavior characteristic for the disordered or weakly separated states and for the microphase-separated states at temperatures above and below the transition, respectively. It is seen in Figure 7 that the bond relaxation times remain almost uninfluenced by the phase separation. This is valid for both symmetric and asymmetric copolymer systems under the condition assumed here that the mobilities of both species A and B are identical. The relaxation time distributions of the end-to-end vectors of blocks in the symmetric copolymer broaden in the vicinity of the ODT and become bimodal below the ODT. In the case of the asymmetric diblock system (Figure 8) the relaxation time spectra for the two blocks differing in length are shown separately. There is a slight difference in the behavior of the two blocks just above the ODT, i.e., in the weak separation regime. A broadening of the spectrum is observed for the longer block whereas the shorter block shows already a distinct bifurcation of the relaxation time spectrum. The dynamic behavior of the whole chains and the effects observed in the relaxations of the concentration correlation are similar for both symmetric and asymmetric diblock systems.

In Figure 9, the temperature dependencies of all relaxation times are shown for symmetric (Figure 9a) and asymmetric (Figure 9b) copolymers. It is seen that the two characteristic temperatures distinguished on the basis of the static and thermodynamic behavior of systems are reflected in the dynamic behavior, as well. Above T_1, the relaxation times remain almost constant.

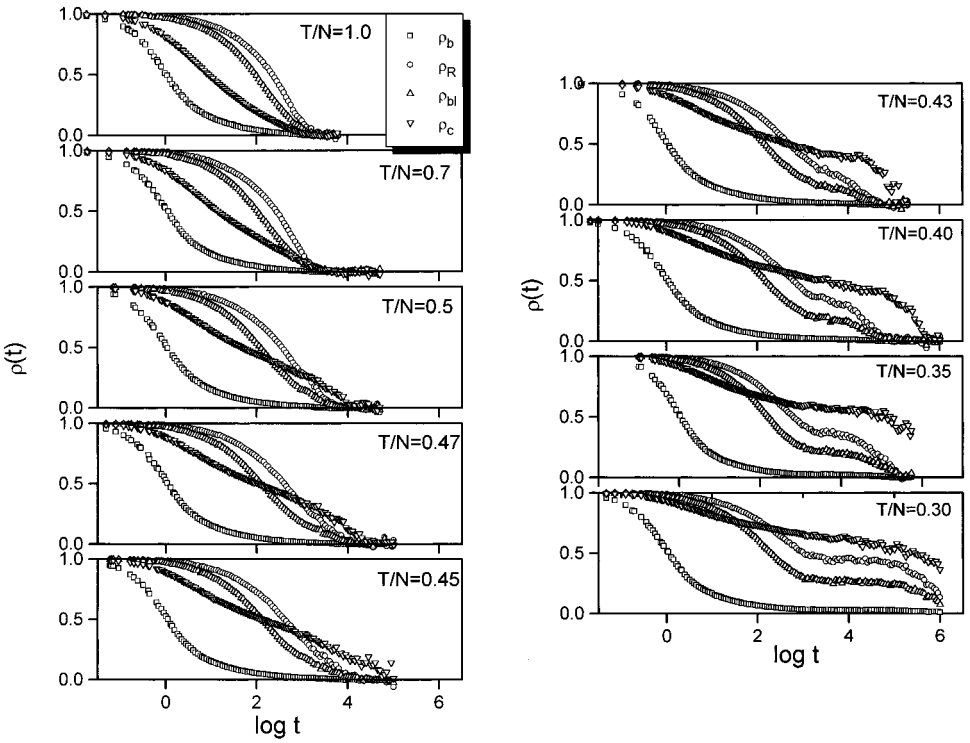

Figure 6. Various correlation functions determined at various temperatures (T/N) for the simulated system of a diblock copolymer melt with $N = 40$ and composition $f = 0.5$. (ρ_b = bond autocorrelation functions (eq 8); ρ_R = end-to-end vector autocorrelation functions (eq 9); ρ_{bl} = block end-to-end vector autocorrelation (eq 10); ρ_c = single point concentration correlation function (eq 11)).

Within the temperature range between T_1 and T_2 important changes are observed in the concentration relaxation times and in the relaxation times of blocks. The splitting of the block end-to-end orientation correlation below T_1 is a very interesting feature; it has not been predicted by the theoretical approach used for the consideration of the end-to-end vector relaxation that has been presented before,[21] which predicts an increased broadening of the distribution of relaxation times in the proximity to the ODT only when the two blocks have different mobilities. For the system simulated here, where there is no difference in the mobilities of the two species, no extra broadening has been expected.

The block end-to-end orientation correlation functions are of special interest for this paper because they can be compared to relaxation times determined experimentally, from the so-called normal mode relaxation in the dielectric spectra.[22] Above T_1, the block relaxation is characterized by a single relaxation time because a single-step correlation function has been observed in this temperature range. On the other hand, below T_2, the correlation functions observed were clearly two-step functions and two relaxation times have been determined by the ILT analysis of the correlation functions. In the intermediate region between T_1 and T_2, two relaxations were also obtained from the ILT procedure, with an increasing separation between the two relaxation times by decreasing temperature. The same type of behavior as presented in Figures 6−9 has been observed for systems with different chain lengths when the temperature scale has been normalized by N.

IV. Discussion

The results presented so far reflect only the effect of A−B repulsive interactions on the dynamics. Throughout the simulations, it has been assumed that the local mobilities of the species are temperature independent; i.e., the bond relaxation is considered as temperature independent and, moreover, the two components A and B that form the two blocks possess the same mobilities. It is known, however, that for the most common diblocks investigated, for example, poly(styrene-*b*-1,4-isoprene),[21,22] the two components possess local frictions differing by factor of 10^6. Even in the homogeneous regime, the presence of concentration fluctuations leads to the existence of two different microenvironments with a difference in the segmental times by factor of 10^4.[19] Moreover, local mobilities have been shown to follow a strong temperature dependence of the well-known Vogel−Fulcher−Tamann (VFT) equation

$$\tau_o = A \exp\left[\frac{B}{T - T_o}\right] \tag{14}$$

with parameters A, B, and T_o characteristic for the individual polymer. This type of temperature dependence has also been observed in simulated systems under an assumption of activated cooperative rearrangements.[35] In order to have a complete picture of the dynamic behavior of copolymer systems, this type of dependence should be superimposed on the changes caused by the A−B interactions observed here. For different mobilities of components the relaxation times of monomers can be additionally influenced by the concentration fluctuations that change with temperature. Increasing concentration fluctuations with decreasing temperature should lead to an increase of the separation of bond relaxation times toward those characteristic for corresponding components A or B.

In another paper[22] we present experimental results related to the dynamics of diblock PS−PI copolymers, as observed by dielectric spectroscopy, which for this system is detecting mainly the relaxation of strong dipole moments of the isoprene monomers. On the basis of the simulation results, we would like to discuss now

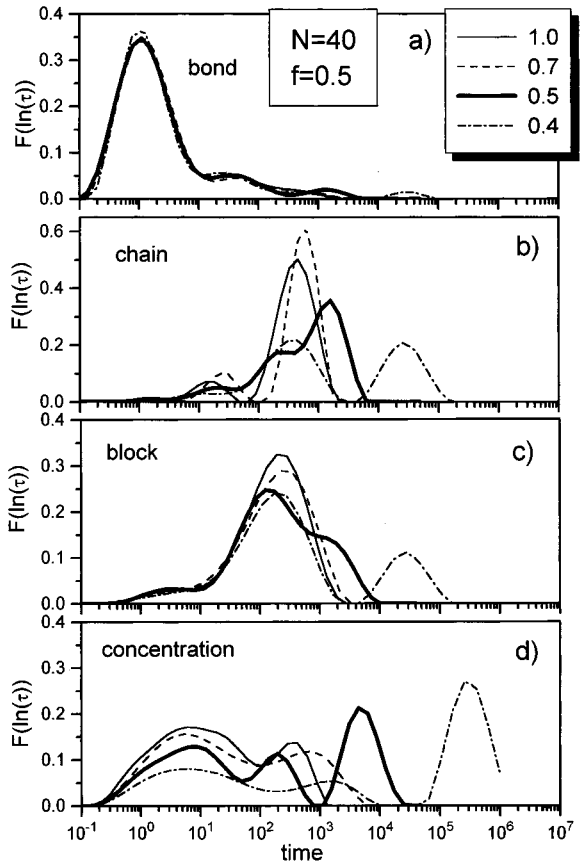

Figure 7. Distribution of relaxation times obtained by inverse Laplace transformation of the calculated correlation functions at various temperatures for the simulated system of a diblock copolymer melt with $N = 40$ and composition $f = 0.5$. Relaxation time distributions of bonds, chains (from chain end-to-end vector autocorrelation function), blocks (from block end-to-end vector autocorrelation), and concentration correlations are shown. Distributions given by thick solid lines correspond to $T/N = 0.5$, the temperature slightly above the ODT.

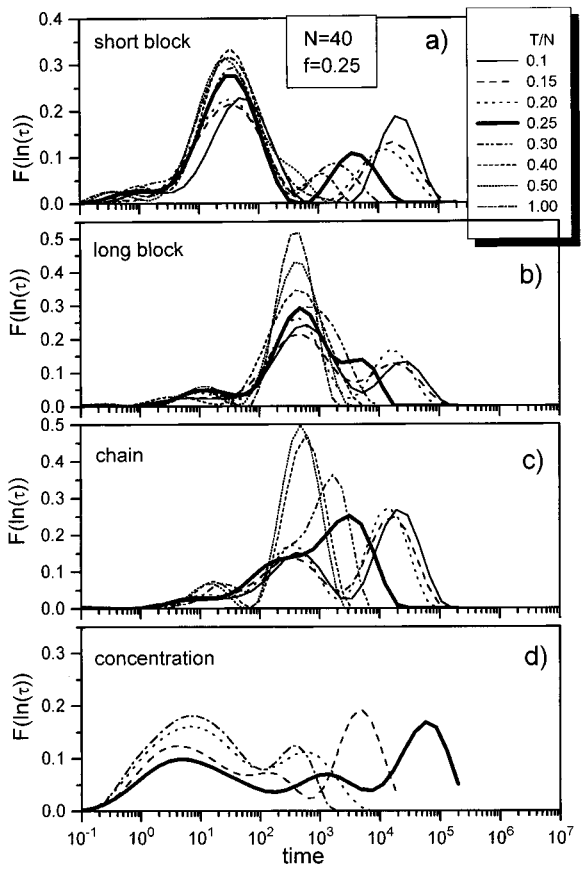

Figure 8. Distribution of relaxation times obtained by inverse Laplace transformation of the calculated correlation functions at various temperatures for the simulated system of a diblock copolymer melt with $N = 40$ and composition $f = 0.25$. Relaxation time distributions of blocks of different lengths, chains, and concentration correlations are shown. Distributions given by thick solid lines correspond to $T/N = 0.25$, the temperature close to the ODT.

which behavior can be expected in such a system when dielectric relaxation effects are detected.

It is known that the specific orientation of dipole moments in the isoprene chain allows an observation of two relaxation modes: the segmental relaxation related to the orientational relaxation of the dipole moment components perpendicular to the chain contour and the relaxation of the whole chain related to the relaxation of the effective dipole moment of the chain that results from the correlation of segmental dipole moment components parallel to the chain contour. The same effects can be expected in diblock copolymers in which one of the blocks consists of isoprene segments with the only difference that the two modes will reflect the behavior of the block instead of the behavior of the whole molecule. However, the behavior of the block will be influenced by the presence of the other component and by the morphological changes in the system.

Considering different mobilities of the components in the PS−PI diblock polymer, we can expect that the relaxation of the isoprene segments will be slowed down in the disordered state where the two kinds of segments are mixed and will almost reach the relaxation rates characteristic for pure isoprene in the microphase-separated states. A crossover between the two regimes should, according to the simulation results, take place between temperatures T_1 and T_2 where the concentration fluctuations change between the two levels characteristic for disordered and strongly separated states. This can lead to a weaker temperature dependence of segmental relaxation times in this temperature range, as one would expect from the single-component VFT dependence. This is illustrated schematically in Figure 10 by means of an activation plot. Consistently with the segmental relaxation, the block relaxation at high temperatures, i.e., in the disordered state of the system, will be shifted along the relaxation time axis according to the ratio of the relaxation times of the block and of the segments (chain length dependent), as observed in the simulation. In this temperature range, it can be assumed that the relaxations of block dipole moments are independent because of noncorrelated orientations of chains. This should change below the temperature T_1 and more drastically below T_2 where the orientation correlations of chain axes and correspondingly of the blocks are indicated by the simulation results. At these temperatures the block dipoles can be regarded as consisting of two components parallel and perpendicular to the direction of local orientation correlation. We can expect that the relaxation of the block dipoles will split to a faster relaxation of uncorrelated perpendicular components and to a slower relaxation of correlated parallel components. The latter will contribute to a local spatial effective dipole moment along the local orientation correlation direction. In particular, below the T_2, where the block orientation correlation direction is uniquely normal to the interface, the correlated block dipole moment components will contribute to an effective dipole moment related to the interface. The relax-

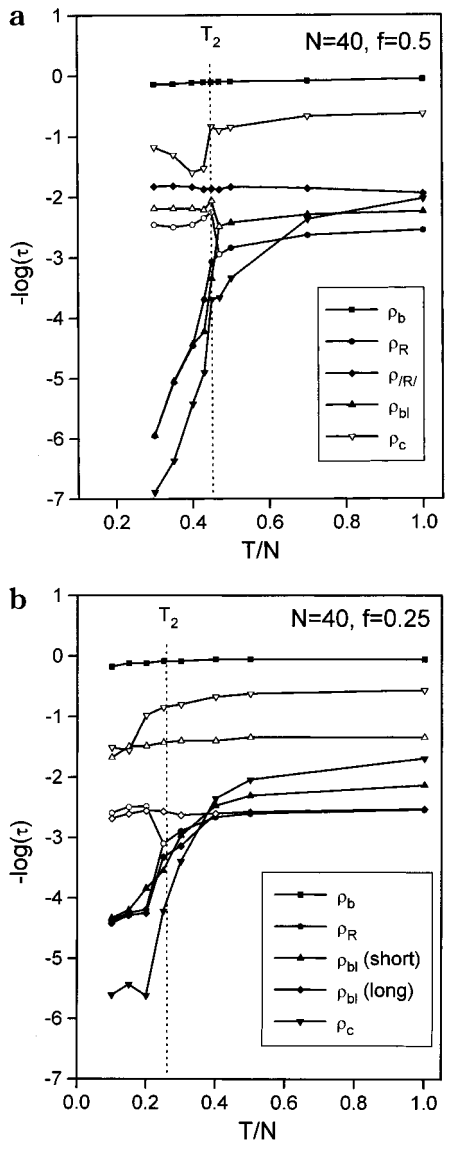

Figure 9. Maps of relaxation times determined at various temperatures (a) for the simulated symmetric diblock copolymer melt with chain length $N = 40$ and composition $f = 0.5$ and (b) for the asymmetric diblock copolymer melt with $N = 40$ and $f = 0.25$. T_1 and T_2 are characteristic temperatures related to the thermodynamic behavior of the system (compare Figures 1 and 2). Various relaxation times are obtained from fits of the simulated correlation functions by a sum of stretched exponential dependencies (eq 13). Open and filled symbols of the same shape describe relaxation times of the fast and slow mode, respectively, when a given correlation function has been described by a sum of two stretched exponential functions. When a single stretched exponential fit was possible the relaxation time of the single mode is shown by means of a filled symbol (see legends).

ation should reflect the extremely slow relaxation of the interfaces, as observed by the slow component of the block relaxation in the simulated systems. These effects should lead to three relaxation modes in the dielectric spectrum that can be expected for the diblock copolymer system below T_2 (ODT): the high-frequency segmental mode and the two slower modes resulting from the bifurcation of the block relaxation into two components, the faster uncorrelated with the interface and the slower corresponding to the interface relaxation. The latter can be extremely slow because it is controlled by the dynamics of the slower component and related to relaxation of large objects greatly exceeding molecular sizes. In the region between temperatures T_1 and T_2

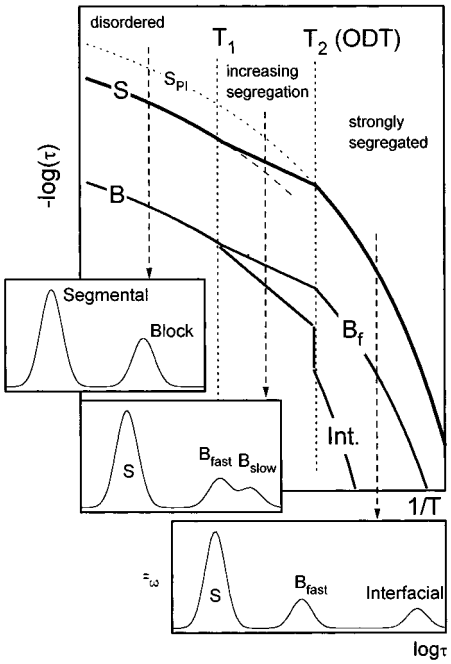

Figure 10. Schematic illustration of the expected dynamic behavior of a diblock copolymer system when observed by the dielectric spectroscopy. It is assumed that dielectric properties of block A are like those for the polyisoprene block in real systems. The VFT temperature dependence is assumed for the pure component A. The solid line S represents the expected temperature dependence of the segmental mode in the copolymer. This relaxation corresponds in the microphase-separated state (below T_2) to the segmental relaxation of the pure component (denoted by S_{PI}). In the disordered state, it is influenced by the other component B, which, as assumed here, slows down the segmental relaxation of A. The solid line B represents the behavior of the normal mode of block A. It bifurcates when the microphase separation in the system takes place. In the strong segregation limit (below T_2) the slow mode is related to the relaxation of the interface. The insets illustrate expected dielectric spectra (ϵ'') in the log τ scale, as characteristic to various temperature regimes.

some intermediate situation can be expected in which a limited correlation of chain orientations can involve only a broadening of the block relaxation mode or a weak separation between the slow and fast components at temperatures closer to T_2. According to the simulation results, the fast component of the block relaxation should remain at approximately constant distance from the segmental mode over the whole temperature range whereas the slow mode can show much stronger temperature dependence especially signified by a drastic change of the relaxation time around T_2.

All the effects discussed above are schematically illustrated in Figure 10. The experimental results presented in another paper[22] have confirmed qualitatively many elements of the picture drawn above. Both the broadening of the normal mode relaxation above the ODT and an extra slow mode below the ODT have been observed for PS−PI block copolymers.

V. Conclusions

The results presented in this paper demonstrate that very detailed information about the structure, thermodynamics, and dynamic properties of block copolymer systems can be obtained from analysis of simplified systems simulated by the cooperative motion algorithm. The method appears effective in simulation of systems within a very broad temperature range, including both the disordered and microphase-separated states. The

results concerning dynamic properties can describe a similar behavior of the simulated systems, as recently observed by the dielectric spectroscopy for polystyrene−polyisoprene copolymers.

Acknowledgment. S.H.A. would like to acknowledge that part of this research was sponsored by NATO's Scientific Affairs Division in the framework of the Science for Stability Programmed and by the Greek General Secretariat of Research and Technology. G.F. and T.P. acknowledge partial support of the Alexander von Humboldt Foundation under Grant Number FOK-OOP USS1685.

References and Notes

(1) Bates, F. S.; Fredrickson, G. H. *Annu. Rev. Phys. Chem.* **1990**, *41*, 525.
(2) *Thermoplastic Elastomers—A Comprehensive Review*; Legge, R., Holden, N. R., Schroeder, H. E., Eds.; Hanser Publishers: Munich, 1988. *Developments in Block Copolymers—II*; Goodman, I., Ed.; Applied Science: London, 1985. *Block Copolymers: Science and Technology*; Meier, D. J., Ed.; MMI Press/Harwood Academic Publishers: New York, 1983. *Developments in Block Copolymers—I*; Goodman, I., Ed.; Applied Science: London, 1982.
(3) Hashimoto, T.; Todo, A.; Itoi, H.; Kawai, H. *Macromolecules* **1977**, *10*, 377. Hashimoto, T.; Shibayama, M.; Kawai, H. *Macromolecules* **1980**, *13*, 1237. Hashimoto, T.; Tanaka, H.; Itoi, H.; Hasegawa, H. *Macromolecules* **1985**, *18*, 1864.
(4) Bates, F. S.; Rosedale, J. H.; Fredrickson, G. H. *J. Chem. Phys.* **1990**, *92*, 6255. Rosedale, J. H.; Bates, F. S. *Macromolecules* **1990**, *23*, 2329.
(5) Bates, F. S.; Rosedale, J. H.; Fredrickson, G. H.; Glinka, C. J. *Phys. Rev. Lett.* **1988**, *61*, 2229. Owens, J. N.; Gancarz, I. S.; Koberstein, J. T.; Russell, T. P. *Macromolecules* **1989**, *22*, 3380. Almdal, K.; Rosedale, J. H.; Bates, F. S.; Wignall, G. D. *Phys. Rev. Lett.* **1990**, *65*, 1112.
(6) Anastasiadis, S. H.; Russell, T. P.; Satija, S. K.; Majkrzak, C. F. *Phys. Rev. Lett.* **1989**, *62*, 1852. Anastasiadis, S. H.; Russell, T. P.; Satija, S. K.; Majkrzak, C. F. *J. Chem. Phys.* **1990**, *92*, 5677. Menelle, A.; Russell, T. P.; Anastasiadis, S. H.; Satija, S. K.; Majkrzak, C. F. *Phys. Rev. Lett.* **1992**, *68*, 67.
(7) Leibler, L. *Macromolecules* **1980**, *13*, 1602.
(8) Fredrickson, G. H.; Helfand, E. *J. Chem. Phys.* **1987**, *87*, 697. Barrat, G. L.; Fredrickson, G. H. *J. Chem. Phys.* **1991**, *95*, 1282.
(9) Semenov, A. N. *Zh. Eksp. Teor. Fiz.* **1985**, *88*, 1242; *Soviet Phys. JETP* **1985**, *61*, 733.
(10) Olvera de la Cruz, M. *Phys. Rev. Lett.* **1991**, *67*, 85.
(11) Helfand, E.; Wasserman, Z. R. In *Developments in Block Copolymers—I*; Goodman, I., Ed.; Applied Science: London, 1982. Meier, D. J. In *Thermoplastic Elastomers—A Comprehensive Review*; Legge, R., Holden, N. R., Schroeder, H. E.; Eds.; Hanser Publishers: Munich, 1988.
(12) Benoit, H.; Hadziioannou, G. *Macromolecules* **1988**, *21*, 1449.
(13) Fried, H.; Binder, K. *Europhys. Lett.* **1991**, *16*, 237; *J. Chem. Phys.* **1991**, *94*, 8349.
(14) Binder, K.; Fried, H. *Macromolecules* **1993**, *26*, 6878.
(15) Gauger, A.; Weyersberg, A.; Pakula, T. *Makromol. Chem., Theory Simul.* **1987**, *2*, 531. Weyersberg, A.; Vilgis, T. A. *Phys. Rev. E* **1993**, *48*, 377.
(16) Larson, R. G. *Macromolecules* **1994**, *27*, 4198.
(17) Fytas, G.; Anastasiadis, S. H. In *Disorder Effects on Relaxation Processes*; Richert, R., Blumen, A., Eds.; Spinger Verlag: Berlin, 1993.
(18) Borsali, R.; Benoit, H.; Legrand, J.-F.; Duval, M.; Picot, C.; Benmouna, M.; Farago, B. *Macromolecules* **1989**, *22*, 4119. Duval, M.; Picot, C.; Benoit, H.; Borsali, R.; Benmouna, M.; Lartigue, C. *Macromolecules* **1991**, *24*, 3185.
(19) Quan, X.; Johnson, G. E.; Anderson, E. W.; Bates, F. S. *Macromolecules* **1989**, *22*, 2451. Kanetakis, J.; Fytas, G.; Kremer, F.; Pakula, T. *Macromolecules* **1992**, *25*, 3484. Rizos, A.; Fytas, G.; Roovers, J. C. *J. Chem. Phys.* **1992**, *97*, 6925.
(20) Alig, I.; Kremer, F.; Fytas, G.; Roovers, J. C. *Macromolecules* **1992**, *25*, 5277. Stuhn, B.; Stickel, F. *Macromolecules* **1992**, *25*, 5306. Yao, M.-L.; Watanabe, H.; Adachi, K.; Kotaka, T. *Macromolecules* **1991**, *24*, 2955. Yao, M.-L.; Watanabe, H.; Adachi, K.; Kotaka, T. *Macromolecules* **1992**, *25*, 1699.
(21) Karatasos, K.; Anastasiadis, S. H.; Semenov, A. N.; Fytas, G.; Pitsikalis, M.; Hadjichristidis, N. *Macromolecules* **1994**, *27*, 3543.
(22) Karatasos, K.; Anastasiadis, S. H.; Floudas, G.; Fytas, G.; Pispas, S.; Hadjichristidis, N.; Pakula, T. *Macromolecules* **1996**, *29*, 1326.
(23) Balsara, N. P.; Stepanek, P.; Lodge, T. P.; Tirrell, M. *Macromolecules* **1991**, *24*, 6227. Balsara, N. P.; Eastman, C. E.; Foster, M. D.; Lodge, T. P.; Tirrell, M. *Makromol. Chem., Macromol. Symp.* **1991**, *45*, 213. Lodge, T. P.; Xu, X.; Jin, X.; Dalvi, M. C. *Macromol. Symp.* **1994**, *87*, 107. Pan, C.; Maurer, W.; Liu, Z.; Lodge, T. P.; Stepanek, P.; von Meerwall, E. D.; Watanabe, H. *Macromolecules* **1995**, *28*, 1643.
(24) Anastasiadis, S. H.; Fytas, G.; Vogt, S.; Fischer, E. W. *Phys. Rev. Lett.* **1993**, *70*, 2415.
(25) Vogt, S.; Anastasiadis, S. H.; Fytas, G.; Fischer, E. W. *Macromolecules* **1994**, *27*, 4335. Jian, T.; Anastasiadis, S. H.; Semenov, A. N.; Fytas, G.; Adachi, K.; Kotaka, T. *Macromolecules* **1994**, *27*, 4762. Fytas, G.; Anastasiadis, S. H.; Semenov, A. N. *Makromol. Chem., Macromol. Symp.* **1994**, *79*, 117.
(26) Jian, T.; Semenov, A. N.; Anastasiadis, S. H.; Fytas, G.; Feh, F.-J.; Chu, B.; Vogt, S.; Wang, F.; Roovers, J. E. L. *J. Chem. Phys.* **1994**, *100*, 3286.
(27) Akcasu, A. Z.; Benmouna, M.; Benoit, H. *Polymer* **1986**, *27*, 1935. Akcasu, A. Z.; Tombakoglu, M. *Macromolecules* **1990**, *23*, 607. Akcasu, A. Z. *Macromolecules* **1991**, *24*, 2109. Borsali, R.; Vilgis, T. A. *J. Chem. Phys.* **1990**, *93*, 3610.
(28) Fredrickson, G. H.; Helfand, E. *J. Chem. Phys.* **1988**, *89*, 5890.
(29) Larson, R. G.; Fredrickson, G. H. *J. Chem. Phys.* **1987**, *86*, 1553.
(30) Benmouna, M.; Vilgis, T. A. *Makromol. Chem., Theory Simul.* **1992**, *1*, 333. Genz, U.; Vilgis, T. A. *J. Chem. Phys.* **1994**, *101*, 7111.
(31) Vilgis, T. A.; Weyersberg, A.; Brereton, M. G. *Phys. Rev. E* **1994**, *49*, 3031.
(32) Brereton, M. G.; Vilgis, T. A. *Macromolecules* **1996**, *29*, 7588.
(33) Pakula, T. *Macromolecules* **1987**, *20*, 679.
(34) Pakula, T.; Geyler, S. *Macromolecules* **1987**, *20*, 2909.
(35) Kirst, K. U.; Kremer, F.; Pakula, T.; Hollingshurst, J. *Colloid Polym. Sci.* **1994**, *272*, 1420.
(36) Pakula, T.; Geyler, S.; Edling, T.; Boese, D. *Rheol. Acta* **1996**, *35*, 631.
(37) Flory, P. J. In *The Principles of Polymer Chemistry*; Cornell University Press, Ithaca, NY, 1953.
(38) Provencher, S. W. *Comput. Phys. Commun.* **1982**, *27*, 213, 229.
(39) Fytas, G.; Meier, G. In *Dynamic Light Scattering*; Brown, W., Ed.; Oxford University Press: Oxford, U.K., 1993; Chapter 9, p 407.

MA9605107